ISSN No:-2456-2165 https://doi.org/10.38124/ijisrt/26nov866

Phase-Level Structural and Compositional Characterization of 3 mol% Ag-Modified ZnO Synthesized Using Neem Leaf Extract

Sadiq Lawan Mahe[1*]; Huzaifa Ali Saleh[1]; Hamza Mustapha Umar[1,2]; Akhilesh Dwivedi[1]; Ibrahim Abba Ibrahim[1]; Nasiru Abdullahi Lawan[1]

[1]Department of Physics, Mewar University, Chittorgarh, Rajasthan, India
[2]Department of Physics, Northwest University Kano, Nigeria

Corresponding Author: Sadiq Lawan Mahe[*]

Publication Date: 2026/11/26

Abstract: Phase composition, distribution of Ag and the structure of the interfaces between the two phases are important factors that should be considered for the accurate characterization of green-synthesized Ag/ZnO heterophases since they are crucial in the interpretation of the physicochemical and potential functional properties of this system. This study investigates one of the formulation samples (S2) with nominal composition 3 mol% Ag/Zn and prepared by zinc acetate, AgNO3 and Azadirachta indica (Neem) leaf extract. The material was characterized by X-ray diffraction (XRD), scanning electron microscopy (SEM), energy-dispersive X-ray spectroscopy (EDX) and Fourier-transform infrared spectroscopy (FTIR). XRD identified the presence of crystalline hexagonal wurtzite ZnO and further reflections were observed at around 37.185°, 43.365°, 63.555°, and 76.515° that would be consistent with a crystalline Ag-containing phase. The resultant refined diffraction pattern showed provisional lattice parameters for ZnO of a = 0.3250 nm and c = 0.5202 nm and apparent crystallite size of ≈17.13 nm and apparent micro strain of ≈2.90 × 10−5. Local compositional variation was observed, with 1.11 at% Ag being identified by EDX at one analyzed position, and Ag below detection at a second position. The SEM results revealed the presence of high degree of agglomeration and irregular clustered morphology. Vibrational features associated with the Zn–O-region and surface-associated vibrational features were identified by FTIR. The datasets, combined, provide a phase line description of S2 as a nominal 3 mol% Ag modified ZnO material with evidence of a separate crystalline Ag containing phase. The analysis is split into direct observations, and structural assignments that need more spatially and chemically resolved measurements. The present dataset does not establish substitutional or interstitial Ag incorporation, the oxidation state of Ag or uniform atomic-level distribution of Ag, nor a specific nanoscale architecture.

How to Cite: Sadiq Lawan Mahe; Huzaifa Ali Saleh; Hamza Mustapha Umar; Akhilesh Dwivedi; Ibrahim Abba Ibrahim; Nasiru Abdullahi Lawan (2026) Phase-Level Structural and Compositional Characterization of 3 mol% Ag-Modified ZnO Synthesized Using Neem Leaf Extract. *International Journal of Innovative Science and Research Technology*, 11(11), 1772-1780. https://doi.org/10.38124/ijisrt/26nov866

I. INTRODUCTION

Zinc oxide is a technologically important semiconductor whose crystalline structure, surface chemistry, morphology, and defect characteristics influence its physicochemical behavior and suitability for applications including photocatalysis, sensing, antimicrobial systems, and related functional materials [1]. Modification of ZnO with Ag has attracted substantial interest because Ag can coexist with ZnO in structurally distinct configurations, including systems in which crystalline Ag is present as a separate phase [2-6].

Interpreting Ag-containing ZnO requires a distinction between detecting Ag and demonstrating its incorporation into the ZnO lattice. Additional Ag diffraction reflections can provide evidence for a crystalline Ag phase, whereas changes in ZnO diffraction positions or lattice parameters have been used in some studies to discuss possible Ag incorporation [3–7]. EDX establishes Ag within the analyzed region but does not independently determine its atomic position in ZnO [2-3]. SEM shows morphology, agglomeration, and apparent heterogeneity, but cannot determine whether Ag is substitutionally incorporated. FTIR adds vibrational and surface-chemical information without independently resolving the atomic position of Ag.

Previous investigations have examined Ag/ZnO materials using complementary structural, morphological, elemental, and vibrational techniques [2–7]. Their structural interpretations are not necessarily equivalent. Some studies identify metallic Ag as a distinct crystalline phase, whereas others discuss changes in ZnO structural parameters as

ISSN No:-2456-2165 https://doi.org/10.38124/ijisrt/26nov866

evidence consistent with Ag incorporation [3-8]. The terms Ag-doped and Ag-modified ZnO therefore do not, by themselves, establish whether Ag occupies the ZnO lattice or occurs partly as a separate Ag-containing phase.

Green synthesis using plant extracts provides an alternative route for preparing ZnO and Ag/ZnO materials [9-11]. Neem-mediated ZnO synthesis has been reported using complementary physicochemical characterization, including FTIR, XRD, SEM, and EDX/EDAX [10-11]. Ag/ZnO materials prepared through biological or green routes have also been reported, showing that plant-derived systems can produce materials in which ZnO and Ag-related phases can be investigated together [2], [12], [5], [6].

Despite the extensive literature on Ag-modified ZnO, distinguishing crystalline Ag-phase formation from presumed atomic incorporation remains important. The present study focuses on one characterized sample, S2, rather than presenting a concentration-series investigation. The available XRD, EDX, SEM, and FTIR evidence is integrated to establish the strongest defensible phase-level structural designation without exceeding what the measurements can support.

The study integrates the XRD, EDX, SEM, and FTIR evidence for S2 to distinguish evidence for a crystalline Ag-containing phase from claims of substitutional or interstitial Ag incorporation that cannot be established by the available techniques.

II. EXPERIMENTAL METHODS

➢ *S2 Sample and Synthesis*

S2 represents the nominal 3 mol% Ag/Zn formulation. For 100 mL of a 0.1 mol L^{-1} zinc precursor solution, 2.195 g of zinc acetate dihydrate was used and 0.051 g AgNO3 was used as the Ag precursor. The AgNO3 was dissolved separately in 10 mL deionized water before combination with the zinc precursor. Neem leaf extract was used at 20 mL per 100 mL metal solution. The synthesis pH was adjusted to 10–12 using 1 mol L^{-1} NaOH, followed by heating at 60–80 °C for 2–3 h under stirring at approximately 6.67–8.33 s^{-1}. The product was recovered by centrifugation at approximately 83.3 s^{-1} for 15 min, washed three times with deionized water and once with ethanol, dried at 80–100 °C overnight, and calcined at 400–500 °C for 2–3 h.

Only the characterized S2 sample is considered in this manuscript. The original experimental design included other Ag loadings, but no characterization results from those samples are used here and no concentration-dependent conclusions are drawn. Figure 1 summarizes the synthesis sequence.

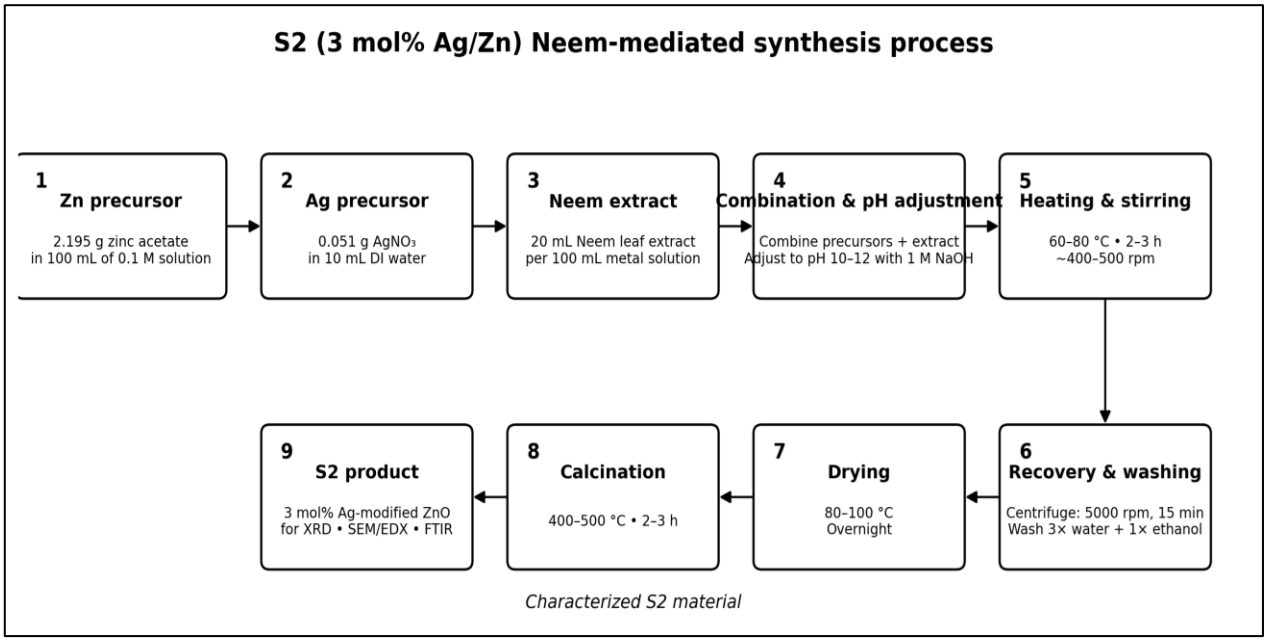

Fig 1 S2 Synthesis Workflow Based Only on the Experimental Conditions Reported in this Study.

➢ *Characterization*

S2 was characterized using XRD, SEM, EDX, and FTIR. XRD was used to identify crystalline phases and evaluate peak positions and broadening. SEM was used to assess surface morphology and agglomeration. EDX was used to determine local elemental composition at the analyzed positions. FTIR was used to examine principal vibrational and surface-associated spectral features. Instrument-specific acquisition parameters are reported only where they are supported by the available experimental record.

➢ *Quantitative XRD Analysis*

The refined XRD dataset contained seven ZnO reflections and four Ag-related reflections. ZnO lattice parameters were calculated from the refined diffraction positions after application of an internally estimated 2θ offset. Williamson–Hall analysis was used to obtain an apparent crystallite size and apparent micro strain, following the

ISSN No:-2456-2165 https://doi.org/10.38124/ijisrt/26nov866

conventional size–strain approach [13], [14]. Because no independent reference-standard calibration or instrumental broadening function was available, the angular correction and broadening-derived quantities are treated as provisional/apparent parameters rather than fully calibrated intrinsic values.

➢ *Evidence Hierarchy*

The interpretation distinguishes direct observations from literature-supported interpretations, provisional quantitative parameters, and claims that cannot be established by the present dataset. This prevents elemental detection, morphology, or vibrational features from being converted into unsupported atomic-scale structural claims. Table 1 presents available experimental evidence for S2.

Table 1 Available Experimental Evidence for S2.

Technique	S2 observation	Evidence status
XRD	Crystalline ZnO reflections; additional reflections at 37.185°, 43.365°, 63.555°, 76.515°	Direct phase evidence; Ag assignment requires validation
EDX	Position 1: Ag 0.00, O 51.69, Zn 48.31 at%; Position 2: Ag 1.11, O 45.71, Zn 53.18 at%	Direct local elemental evidence
SEM	Pronounced agglomeration; irregular/clustered morphology	Direct morphological evidence
FTIR	Bands near 3402, 1429, 991, 881, 687, 417 and 403 cm^{-1}	Direct spectral observation; assignments are constrained

III. RESULTS AND DISCUSSION

➢ *XRD: Phase Identification*

The XRD pattern of S2 contains the principal reflections expected for crystalline hexagonal wurtzite ZnO. The refined ZnO reflections occur at 30.795°, 33.495°, 35.295°, 46.695°, 55.695°, 61.995°, and 67.065°. These reflections correspond to the (100), (002), (101), (102), (110), (103), and (112) planes, respectively, and establish the presence of crystalline ZnO. The measured profile is shown in Figure 2.

Four additional reflections occur at 37.185°, 43.365°, 63.555°, and 76.515°. These positions are consistent with the (111), (200), (220), and (311) reflections associated with face-centered-cubic Ag when the measurement/reference position is considered. Similar identification of crystalline Ag alongside ZnO has been reported in Ag/ZnO systems [2-6]. In S2, the assignment is described as evidence consistent with a separate crystalline Ag-containing phase because the internal angular correction and phase matching have not been independently validated.

Figure 2 and Figure 3 demonstrate raw experimental XRD intensity profile of S2. The trace is plotted directly from the measured dataset without artificial smoothing or reconstructed intensity and XRD peak positions used for internal phase comparison. Solid lines denote reported/refined positions and dashed lines show the internally estimated +0.9095° correction. The correction is not an independent instrument calibration.

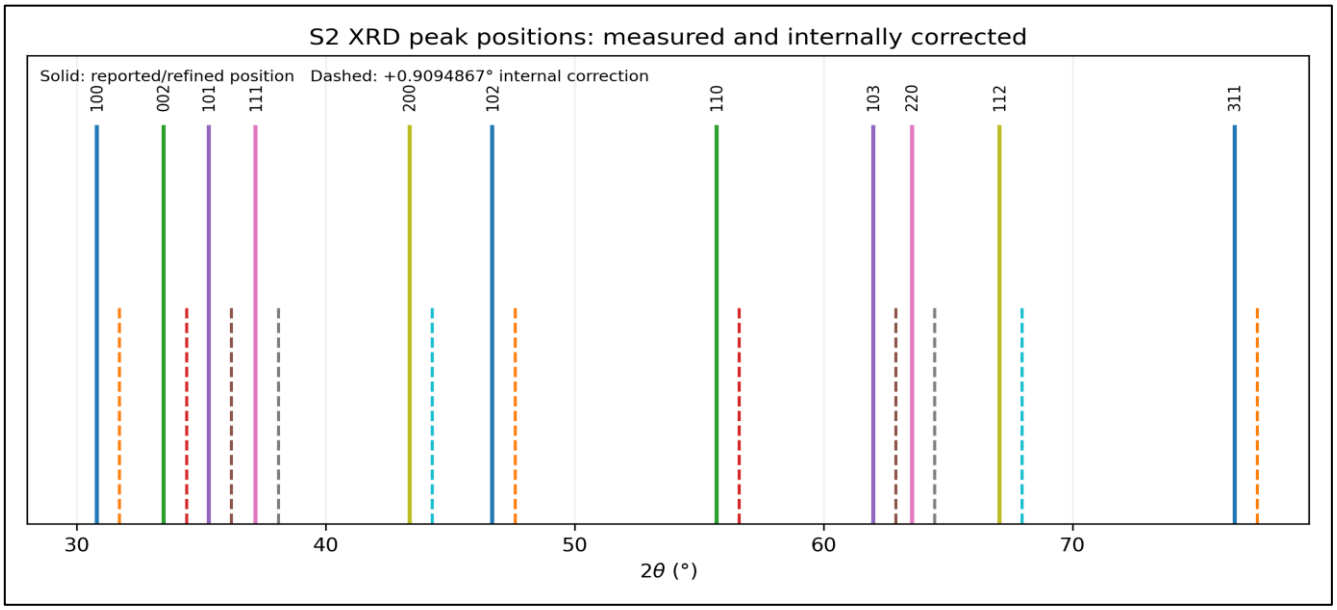

Fig 2 Illustrates the Raw Experimental XRD Intensity Profile of S2. The Trace is Plotted Directly from the Measured Dataset without Artificial Smoothing or Reconstructed Intensity.

ISSN No:-2456-2165 https://doi.org/10.38124/ijisrt/26nov866

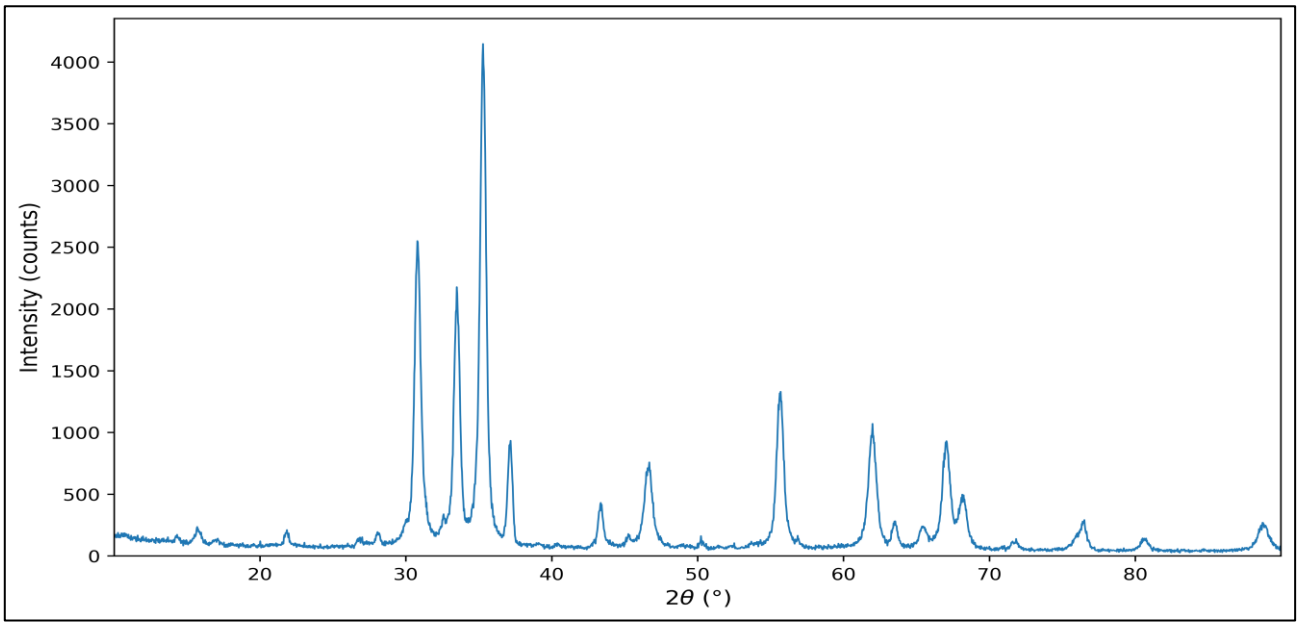

Fig 3 XRD Peak Positions Used for Internal Phase Comparison. Solid Lines Denote Reported/Refined Positions and Dashed Lines Show the Internally Estimated +0.9095° Correction. The Correction is not an Independent Instrument Calibration.

➢ *SEM: Morphology and Agglomeration*

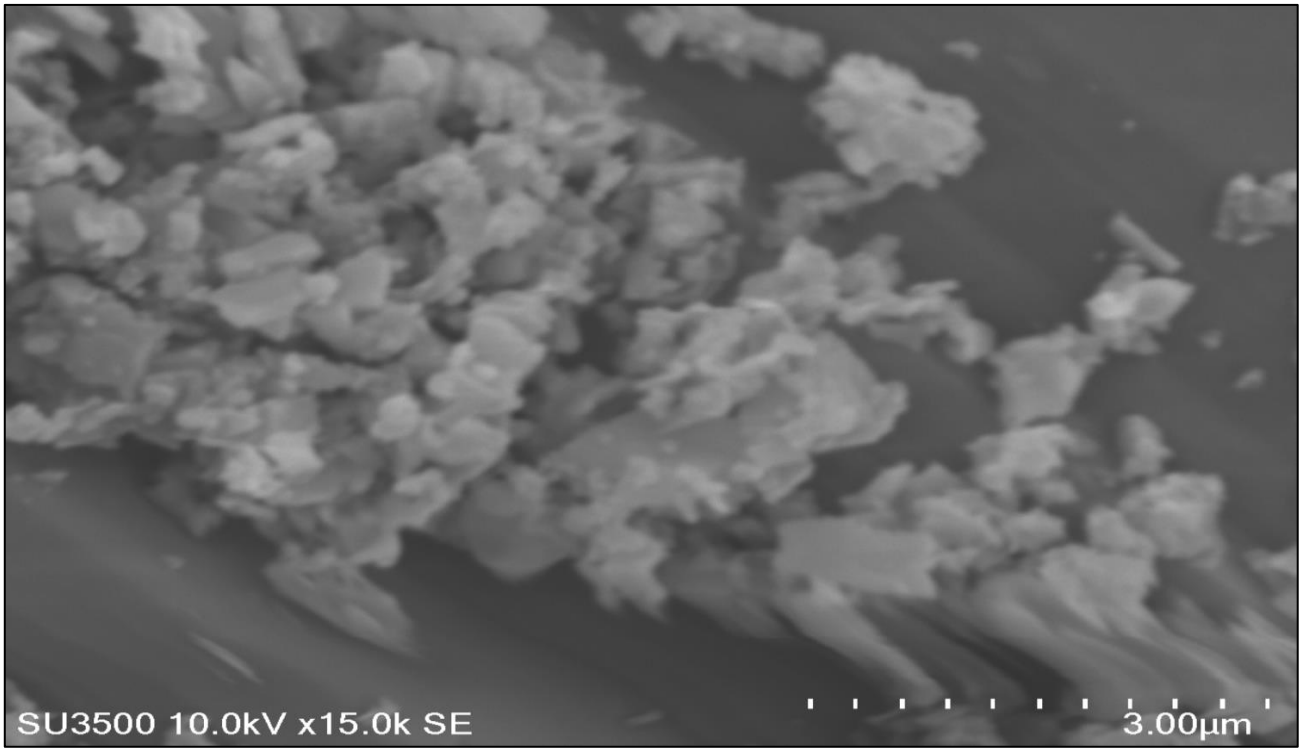

Fig 4 Proves the Actual S2 SEM Micrograph Acquired at 15.0k× in Secondary-Electron Mode. The Image Shows Pronounced Agglomeration and Irregular Clustered Morphology; the 3.00 µm Scale Bar is Visible in the Original Micrograph.

The SEM micrograph of S2 shows pronounced agglomeration, with irregular and clustered structures distributed across the observed field. The image was acquired at 15.0k× in secondary-electron mode, and the original micrograph includes a 3.00 µm scale bar. Individual particle boundaries are not sufficiently separated in the available image to support reliable primary-particle size measurements. The observed features are therefore described as agglomerated or clustered morphology rather than assigned a nanoparticle diameter from the SEM image. Figure 4 shows the corresponding micrograph.

The SEM appearance should be considered separately from the crystallite size obtained from XRD. XRD-derived crystallite size refers to coherently diffracting domains, whereas the structures visible by SEM may represent larger

ISSN No:-2456-2165 https://doi.org/10.38124/ijisrt/26nov866

particles or aggregates. The morphology of ZnO-based materials can vary with synthesis and post-treatment conditions [1], [8], [10]. Accordingly, the dimensions of the agglomerated structures in Figure 4 are not converted into a primary crystallite size.

➢ *EDX: Local Elemental Composition*

EDX measurements show compositional variation between the two analyzed positions on S2. At Position 1, the measured composition is 51.69 at% O and 48.31 at% Zn, with Ag below the reported detection level. Position 2 contains 45.71 at% O, 53.18 at% Zn, and 1.11 at% Ag. The Ag signal at Position 2 therefore confirms that Ag is present within the region examined by EDX.

The difference between the two measurements indicates local compositional variation, but two EDX positions are insufficient to establish macroscopic Ag segregation or a specimen-wide Ag distribution. The 1.11 at% Ag measured at Position 2 should also not be treated as equivalent to the nominal 3 mol% Ag/Zn formulation. The former is a local EDX composition, whereas the latter describes the synthesis formulation. EDX does not determine whether the detected Ag occupies substitutional, interstitial, interfacial, or separate-phase sites [2], [3], [6].

➢ *FTIR: Vibrational and Surface-Chemical Features*

The FTIR spectrum of S2 contains features near 3402, 1429, 991, 881, 687, 417, and 403 cm^{-1}. The broad band around 3402 cm^{-1} is consistent with O–H stretching associated with surface hydroxyl groups and/or adsorbed moisture. The features near 1429, 991, 881, and 687 cm^{-1} occur in regions that may include contributions from surface-associated organic species, carbonate-related species, or other residual components. Without a suitable control spectrum, these bands cannot be assigned more specifically from the S2 spectrum alone.

The feature near 417 cm^{-1} lies within the Zn–O vibrational region reported for Neem-mediated ZnO [11]. The feature near 403 cm^{-1} occurs close to the lower measurement boundary and is therefore not treated as a robust independent band without repeat or control measurements. No Ag-specific FTIR shift is established from the available S2 spectrum. FTIR contributes information about Zn–O-region vibrations and surface-associated chemical features, but it does not establish the atomic position or oxidation state of Ag.

➢ *Integrated XRD–SEM–EDX–FTIR Interpretation*

The four characterization methods provide different pieces of information about S2. XRD identifies crystalline ZnO and shows additional reflections consistent with a crystalline Ag-containing phase. EDX detects Ag at one of the analyzed positions, providing independent local elemental evidence. SEM shows pronounced agglomeration and an irregular clustered morphology, while FTIR provides complementary information from the Zn–O region and surface-associated vibrational features.

Considered together, these results support a phase-level description of S2 in which crystalline ZnO is accompanied by an Ag-containing component consistent with a separate crystalline phase. The datasets do not, however, provide sufficient evidence to determine whether Ag is substitutionally or interstitially incorporated into the ZnO lattice. This distinction is consistent with previous Ag/ZnO studies in which structural, elemental, and morphological measurements have been used to characterize materials containing Ag-associated or heterophase structures [2-6]. Figure 5 summarizes the integrated interpretation.

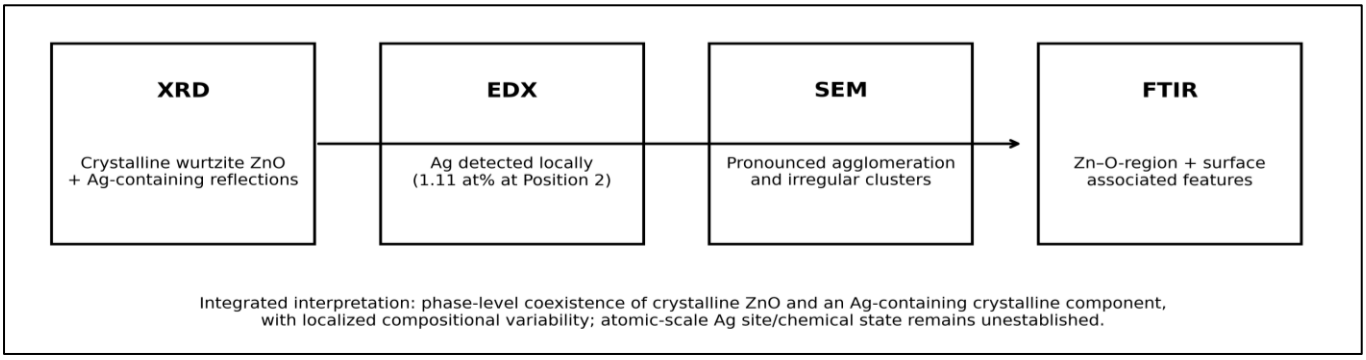

Fig 5 Integrated Evidence Framework for the S2 Characterization. The Diagram Summarizes the Phase-Level Interpretation without Assigning an Atomic Ag Site or Chemical State.

➢ *Evidence-Constrained Structural Interpretation*

The most defensible designation of S2 is a nominal 3 mol% Ag-modified ZnO material exhibiting crystalline ZnO together with evidence consistent with a separate crystalline Ag-containing phase. This interpretation is supported primarily by the XRD and EDX results and remains at the phase level because the available measurements do not resolve the atomic-scale location of Ag.

The term "Ag-modified" is therefore used rather than an unqualified designation of "Ag-doped ZnO." The latter could imply that Ag occupies specific sites within the ZnO lattice, which has not been established for S2. Previous Ag/ZnO studies also show that Ag can occur as a distinct phase, so the terminology is kept consistent with what the available evidence can demonstrate [3]–[7].

ISSN No:-2456-2165 https://doi.org/10.38124/ijisrt/26nov866

➢ *Quantitative XRD*

Quantitative analysis of the refined S2 diffraction pattern gives an internally estimated 2θ offset of 0.9094867°. Applying this correction gives provisional ZnO lattice parameters of a = 0.32498029 nm and c = 0.52019450 nm, with c/a = 1.6006955. The mean lattice parameter calculated from the Ag-related reflections is 0.40866479 ± 0.0001918 nm. Williamson–Hall analysis gives an apparent crystallite size of 17.1288 nm and an apparent micro strain of 2.9027 × 10^{-5}. Figure 3 shows the peak-position comparison used for the internal refinement.

These quantities should be regarded as provisional or apparent parameters. The 0.9095° correction was obtained internally from the present diffraction pattern and was not independently validated against a certified reference standard. Instrumental broadening was also not independently determined. The refined lattice parameters and Williamson–Hall quantities can therefore be used for internal comparison and structural description, but they should not be presented as fully calibrated intrinsic lattice or strain parameters. Williamson–Hall analysis is a recognized approach for separating size and strain contributions in nanocrystalline materials [13-14]. Table 2 presents refined XRD peak data for S2.

Table 2 Refined XRD Peak Data for S2.

Phase	Hkl	Raw 2θ (°)	Applied Δ2θ (°)	Corrected 2θ (°)	Reference 2θ (°)	FWHM (°)	d (nm)
ZnO	(100)	30.795	+0.9095	31.7045	31.7045	0.4867428	0.2820
ZnO	(002)	33.495	+0.9095	34.4045	34.4045	0.4572706	0.2605
ZnO	(101)	35.295	+0.9095	36.2045	36.2045	0.4929430	0.2479
Ag-containing	(111)	37.185	+0.9095	38.0945	38.0945	0.3978026	0.2360
Ag-containing	(200)	43.365	+0.9095	44.2745	44.2745	0.4087848	0.2044
ZnO	(102)	46.695	+0.9095	47.6045	47.6045	0.5665750	0.1909
ZnO	(110)	55.695	+0.9095	56.6045	56.6045	0.5761071	0.1625
ZnO	(103)	61.995	+0.9095	62.9045	62.9045	0.5531753	0.1476
Ag-containing	(220)	63.555	+0.9095	64.4645	64.4645	0.3828000	0.1444
ZnO	(112)	67.065	+0.9095	67.9745	67.9745	0.5279831	0.1378
Ag-containing	(311)	76.515	+0.9095	77.4245	77.4245	0.4955208	0.1232

➢ *Comparison with The Established Literature*

The observations from S2 are broadly consistent with previous Ag/ZnO studies in which Ag has been identified alongside crystalline ZnO. Panchal et al. reported biogenic Ag/ZnO materials using complementary structural, morphological, elemental, and vibrational characterization [2]. Wang et al. investigated Ag-modified ZnO containing dispersed Ag nanoparticles and evaluated the resulting material using structural and morphological evidence [3]. Hosseini et al. and Liu et al. examined the effects of Ag addition on ZnO structural parameters, illustrating that changes in diffraction characteristics can lead to different structural interpretations depending on the supporting evidence [15], [7].

Other studies have reported distinct Ag/ZnO architectures and green-synthesis approaches. These include core–shell Ag/ZnO structures [4], post-annealing and Ag-modification studies [8], green Ag–ZnO synthesis [5], and biological Ag/ZnO materials characterized using combinations of XRD, SEM/TEM, EDX, and FTIR [6]. Neem-mediated ZnO has likewise been examined using XRD, SEM, EDX, and FTIR [11]. Collectively, these studies support the use of complementary characterization while also showing that the presence of Ag does not, by itself, establish its atomic position within ZnO.

The present study does not claim that a nominal 3 mol% Ag/Zn loading is intrinsically novel. Ag-containing ZnO at approximately this loading has already been investigated [3]. The contribution here lies instead in the interpretation of the available S2 dataset. The analysis separates direct evidence for Ag presence and a possible crystalline Ag-containing phase from structural claims, such as substitutional or interstitial incorporation, that cannot be resolved by the available characterization.

➢ *Limitations and Uncertainty*

- *XRD Calibration:*

The internally estimated 2θ correction of approximately 0.9095° was not independently validated against a certified reference standard. The corrected peak positions should therefore be treated as provisional.

- *Peak Broadening:*

Instrumental broadening was not independently determined. Consequently, the Williamson–Hall crystallite size and microstrain are reported as apparent quantities rather than fully corrected intrinsic values.

- *EDX Sampling:*

Only two EDX positions were analyzed. These measurements provide local compositional information but are insufficient to establish the spatial distribution of Ag throughout the specimen.

- *SEM Morphology:*

The available SEM image shows strong agglomeration and irregular clustered structures. The image therefore does not support reliable statistics for primary-particle size.

ISSN No:-2456-2165 https://doi.org/10.38124/ijisrt/26nov866

- *FTIR Interpretation:*

FTIR cannot independently determine the atomic position or oxidation state of Ag. In addition, the 403 cm^{-1} feature lies close to the lower measurement boundary and should not be treated as a robust independent band without repeat or control measurements.

- *Ag-Content Dependence:*

No concentration-dependent structural trend is established in this study because the present analysis is restricted to the characterized S2 sample. The other nominal Ag levels from the original experimental design are not used to support conclusions here.

- *UV–Vis Evidence:*

UV–Vis data are not included in the experimental interpretation because the available file does not constitute a valid S2 UV–Vis dataset.

➢ *Overall Structural Model*

The available evidence supports a constrained structural model for S2. The material can be described as a crystalline ZnO phase accompanied by an Ag-containing component whose additional XRD reflections are consistent with a separate crystalline Ag-containing phase. EDX provides independent local evidence for Ag in the analyzed region, while SEM and FTIR add morphological and vibrational/surface-chemical information.

This model is intentionally limited to the level supported by the available measurements. It does not assign Ag to a specific ZnO lattice site, and it does not require a core–shell structure, uniform Ag decoration, or a particular Ag oxidation state. Establishing any of these features would require additional structural, spatially resolved, or chemical-state-sensitive measurements.

➢ *Ag-Content Dependence: Scope Restriction*

No Ag-content-dependent structural trend is established in the present study. Although the original experimental design included multiple nominal Ag levels, the analysis reported here is restricted to S2 because only S2 has the characterization dataset required for the present interpretation. The manuscript therefore does not infer phase-emergence thresholds, monotonic changes with Ag concentration, or differences among S0, S1, S2, and S3.

➢ *Structure–Composition–Characterization Correlation*

The correlations identified in this study are restricted to S2. XRD establishes the crystalline ZnO phase and shows additional reflections consistent with a crystalline Ag-containing phase. EDX detects Ag locally at one analyzed position, while SEM reveals pronounced agglomeration and an irregular morphology. FTIR adds information from the Zn–O region and from surface-associated vibrational features. Taken together, these observations connect the crystallographic identity, local composition, morphology, and surface chemistry of S2. Each method samples the material differently and provides information at a different level of structural description; the correlation should not be interpreted as evidence that all four techniques probe the same structural feature or the same spatial region.

➢ *Scientific Contribution and Scope*

The available literature indicates that Ag/ZnO synthesis, Ag-containing ZnO at approximately 3 mol% Ag/Zn loading, Ag-related diffraction features, and the use of XRD, SEM, EDX, and FTIR as a characterization combination are not individually novel. The present manuscript therefore does not claim novelty from the synthesis route, Ag loading, or the characterization techniques themselves.

The contribution of the present study is methodological and interpretive. The S2 dataset is examined by separating three levels of evidence: direct detection of Ag, evidence consistent with a separate crystalline Ag-containing phase, and structural claims concerning atomic-scale Ag incorporation that cannot be established from the available measurements. This approach provides a transparent phase-level designation for S2 and limits interpretation to what the characterization data can support.

➢ *Mechanistic Interpretation*

Under the alkaline synthesis conditions, NaOH promotes the formation of zinc hydroxide species that serve as precursors to ZnO during thermal treatment [16]. Heating facilitates precipitation, nucleation, and growth, while subsequent calcination promotes conversion of the hydroxide precursor to crystalline ZnO and removes residual organic components. Neem-derived constituents may also contribute to precursor transformation and surface stabilization, consistent with previous Neem-mediated ZnO studies [10], [11].

For S2, AgNO3 is the Ag precursor. The final material contains detectable Ag, and the additional XRD reflections are consistent with a crystalline Ag-containing phase. The available measurements, however, do not resolve how Ag is reduced, nucleates, grows, attaches at interfaces, or interacts with the ZnO structure during synthesis and calcination. These processes are therefore presented as plausible mechanistic pathways rather than experimentally established atomic-scale events.

The four characterization datasets provide complementary evidence at different levels. XRD establishes crystalline ZnO and identifies additional reflections consistent with a crystalline Ag-containing phase; EDX provides local Ag detection; SEM reveals pronounced agglomeration; and FTIR provides information from the Zn–O region and surface-associated vibrational features. Taken together, these observations support the phase-level interpretation developed for S2 without establishing atomic-scale Ag incorporation.

➢ *Limitations and Future Work*

The internally estimated 2θ correction of approximately 0.9095° was not independently validated against a certified reference standard, and instrumental broadening was not independently determined. The lattice parameters and

ISSN No:-2456-2165 https://doi.org/10.38124/ijisrt/26nov866

Williamson–Hall size–strain quantities should therefore be regarded as provisional or apparent. Only two localized EDX positions were analyzed, limiting conclusions about the spatial distribution of Ag. The strong agglomeration visible in the SEM image also prevents reliable primary-particle size statistics. The FTIR spectrum provides useful information on Zn–O and surface-associated features, but it cannot establish the atomic position or oxidation state of Ag. The 403 cm^{-1} feature lies close to the lower measurement boundary and should be interpreted cautiously.

Future work should include independent XRD calibration using a certified reference material, spatially resolved EDX mapping, and higher-resolution electron microscopy such as TEM/SAED, where available. Chemical-state-sensitive measurements would further constrain the interpretation of Ag, while controlled FTIR comparisons could improve assignment of surface-associated bands. Additional Ag concentrations could be examined in future experiments to establish concentration-dependent trends, but those samples are outside the evidence base of the present manuscript. Functional measurements would also be required to determine whether the phase-level characteristics identified for S2 correspond to measurable application performance.

IV. CONCLUSIONS

This study provides an evidence-constrained characterization of S2, the nominal 3 mol% Ag-modified ZnO material, using XRD, EDX, SEM, and FTIR. The measurements establish crystalline hexagonal wurtzite ZnO, detect Ag locally, show pronounced agglomeration, and reveal Zn–O-region and surface-associated FTIR features.

The additional XRD reflections at 37.185°, 43.365°, 63.555°, and 76.515° are consistent with a crystalline Ag-containing phase. The internally refined ZnO lattice parameters are a = 0.32498 nm and c = 0.52019 nm. Williamson–Hall analysis gives an apparent crystallite size of 17.13 nm and apparent microstrain of 2.90×10^{-5}. These quantitative values remain provisional because the angular correction and instrumental broadening were not independently validated.

EDX detects Ag at one analyzed position but not at another, indicating local compositional variation without establishing macroscopic segregation. SEM confirms strong agglomeration, while FTIR provides complementary vibrational information without establishing Ag-specific bonding, lattice position, or oxidation state.

The strongest supported designation is therefore a nominal 3 mol% Ag-modified ZnO material exhibiting crystalline ZnO together with evidence consistent with a separate crystalline Ag-containing phase. Substitutional or interstitial Ag incorporation into specific ZnO lattice sites is not established by the available characterization.

➢ *Funding*

This research received no specific grant from any funding agency in the public, commercial or not-profits sectors.

➢ *Conflict of interest*

The authors declare no conflict of interest related to this study.

➢ *Data availability*

The experimental XRD, SEM, EDX, and FTIR data supporting the findings of this study, together with the associated synthesis procedure, are available from the corresponding author upon reasonable request.

➢ *Authors Contributions*

- *Sadiq Lawan Mahe:*
  Conceptualization, investigation, writing the original draft
- *Huzaifa Ali Saleh:*
  Methodology, writing, reviewing and editing.
- *Hamza Mustapha Umar:*
  Investigation, resources, writing and reviewing
- *Akhilesh Dwivedi:*
  Data curation, formal analysis, editing.
- *Ibrahim Abba Ibrahim:*
  Resources, validation, software
- *Nasiru Abdullahi Lawan:*
  Literature search and synthesis

➢ *Declarations*

- *Ethical Approval*
  Not applicable
- *Consent to Participate*
  Not applicable
- *Consent to Publish*
  Not applicable

REFERENCES

[1]. Z. Fan and J. G. Lu, “Zinc oxide nanostructures: Synthesis and properties,” Journal of Nanoscience and Nanotechnology, vol. 5, no. 10, pp. 1561–1573, 2005, DOI: 10.1166/jnn.2005.182.

[2]. P. Panchal, D. R. Paul, A. Sharma, P. Choudhary, P. Meena, and S. P. Nehra, “Biogenic mediated Ag/ZnO nanocomposites for photocatalytic and antibacterial activities towards disinfection of water,” Journal of Colloid and Interface Science, vol. 563, pp. 370–380, 2020, DOI: 10.1016/j.jcis.2019.12.079.

ISSN No:-2456-2165 https://doi.org/10.38124/ijisrt/26nov866

[3]. S. Wang, F. Jia, X. Wang, L. Hu, Y. Sun, G. Yin, T. Zhou, Z. Feng, P. Kumar, and B. Liu, "Fabrication of ZnO nanoparticles modified by uniformly dispersed Ag nanoparticles: Enhancement of gas sensing performance," ACS Omega, vol. 5, no. 10, pp. 5209–5218, 2020, DOI: 10.1021/acsomega.9b04243.

[4]. L. Muñoz-Fernandez, G. Alkan, O. Milošević, M. E. Rabanal, and B. Friedrich, "Synthesis and characterization of spherical core-shell Ag/ZnO nanocomposites using single and two-steps ultrasonic spray pyrolysis," Catalysis Today, vol. 321–322, pp. 26–33, 2019, DOI: 10.1016/j.cattod.2017.11.029.

[5]. S. S. Patil, M. G. Mali, M. S. Tamboli, D. R. Patil, M. V. Kulkarni, H. Yoon, H. Kim, S. S. Al-Deyab, S. S. Yoon, S. S. Kolekar, and B. B. Kale, "Green approach for hierarchical nanostructured Ag-ZnO and their photocatalytic performance under sunlight," Catalysis Today, vol. 260, pp. 126–134, 2016, DOI: 10.1016/j.cattod.2015.06.004.

[6]. M. C. Jobe, D. M. N. Mthiyane, M. Mwanza, and D. C. Onwudiwe, "Biosynthesis of zinc oxide and silver/zinc oxide nanoparticles from Urginea epigea for antibacterial and antioxidant applications," Heliyon, vol. 8, no. 12, Art. no. e12243, 2022, DOI: 10.1016/j.heliyon. 2022.e12243.

[7]. F.-C. Liu, J.-Y. Li, T.-H. Chen, C.-H. Chang, C.-T. Lee, W.-H. Hsiao, and D.-S. Liu, "Effect of silver dopants on the ZnO thin films prepared by a radio frequency magnetron co-sputtering system," Materials, vol. 10, no. 7, Art. no. 797, 2017, DOI: 10.3390/ma10070797.

[8]. A. Obeydavi, K. Dastafkan, M. Rahimi, and M. A. G. Dezfouli, "Insights into post-annealing and silver doping effects on the internal microstructure of ZnO nanoparticles through X-ray diffraction probe," Solid State Sciences, vol. 69, pp. 71–81, 2017, DOI: 10.1016/j.solidstatesciences.2017.05.004.

[9]. K. K. Panda, D. Golari, A. Venugopal, V. M. M. Achary, G. Phaomei, N. L. Parinandi, H. K. Sahu, and B. B. Panda, "Green Synthesized Zinc Oxide (ZnO) Nanoparticles Induce Oxidative Stress and DNA Damage in Lathyrus sativus L. Root Bioassay System," Antioxidants, vol. 6, no. 2, Art. no. 35, 2017, DOI: 10.3390/antiox6020035.

[10]. K. Elumalai and S. Velmurugan, "Green synthesis, characterization and antimicrobial activities of zinc oxide nanoparticles from the leaf extract of Azadirachta indica (L.)," Applied Surface Science, vol. 345, pp. 329–336, 2015, DOI: 10.1016/j.apsusc.2015.03.176.

[11]. A. Singh, Neelam, and M. Kaushik, "Physicochemical investigations of zinc oxide nanoparticles synthesized from Azadirachta indica (Neem) leaf extract and their interaction with Calf-Thymus DNA," Results in Physics, vol. 13, Art. no. 102168, 2019, DOI: 10.1016/j.rinp.2019.102168.

[12]. Y. Iqbal, A. R. Malik, T. Iqbal, M. H. Aziz, F. Ahmed, F. A. Abolaban, S. M. Ali, and H. Ullah, "Green synthesis of ZnO and Ag-doped ZnO nanoparticles using Azadirachta indica leaves: Characterization and their potential antibacterial, antidiabetic, and wound-healing activities," Materials Letters, vol. 305, Art. no. 130671, 2021, DOI: 10.1016/j.matlet.2021.130671.

[13]. A. Khorsand Zak, W. H. Abd. Majid, M. E. Abrishami, and R. Yousefi, "X-ray analysis of ZnO nanoparticles by Williamson–Hall and size–strain plot methods," Solid State Sciences, vol. 13, no. 1, pp. 251–256, 2011, DOI: 10.1016/j.solidstatesciences.2010.11.024.

[14]. V. Mote, Y. Purushotham, and B. N. Dole, "Williamson-Hall analysis in estimation of lattice strain in nanometer-sized ZnO particles," Journal of Theoretical and Applied Physics, vol. 6, Art. no. 6, 2012, DOI: 10.1186/2251-7235-6-6.

[15]. S. M. Hosseini, I. A. Sarsari, P. Kameli, and H. Salamati, "Effect of Ag doping on structural, optical, and photocatalytic properties of ZnO nanoparticles," Journal of Alloys and Compounds, vol. 640, pp. 408–415, 2015, DOI: 10.1016/j.jallcom.2015.03.136.

[16]. J. Wang, P. Ma, and L. Xiang, "Effects of NaOH on formation of ZnO nanorods from ε-$Zn(OH)_2$," Materials Letters, vol. 141, pp. 118–121, 2015, DOI: 10.1016/j.matlet.2014.11.081.